Angle-Resolved Linear Dichroism to Probe the Organization of Highly Ordered Collagen Biomaterials

Natacha Krins, Frank Wien, Margaux Schmeltz, Javier Pérez, Dounia Dems, Nicolas Debons, Christel Laberty-Robert, Marie-Claire Schanne-Klein, Carole Aimé

Angle-resolved linear dichroism to probe the organization of highly-ordered collagen biomaterials

Natacha Krins,[a] Frank Wien,[b] Margaux Schmeltz,[c] Javier Pérez,[b] Dounia Dems,[a] Nicolas Debons,[a] Christel Laberty-Robert,[a] Marie-Claire Schanne-Klein,[c] Carole Aimé[a,d]*

a. Sorbonne Université, CNRS, Laboratoire de Chimie de la Matière Condensée de Paris (LCMCP), Paris, F-75005, France

b. SOLEIL Synchrotron, 91190 Saint Aubin, France

c. Laboratoire d'Optique et Biosciences, Ecole Polytechnique, CNRS, Inserm, Institut Polytechnique de Paris, F-91128 Palaiseau, France

d. PASTEUR, Département de chimie, École normale supérieure, PSL University, Sorbonne Université, CNRS, 75005 Paris, France

ABSTRACT. Controlling the assembly of high-order structures is central to soft-matter and biomaterial engineering. Angle-resolved linear dichroism can probe the ordering of chiral collagen molecules in the dense state. Collagen triple helices were aligned by solvent evaporation. Their ordering gives a strong linear dichroism (LD) that changes sign and intensity with varying sample orientations with respect to the beam linear polarization. Being complementary to circular dichroism, which probes the structure of chiral (bio)molecules, LD can shift from the molecular to the supramolecular scale, and from the investigation of the conformation to interactions.

Supported by multiphoton microscopy and X-ray scattering, we show that LD provides a straightforward route to probe collagen alignment, determine the packing density, and monitor denaturation. This approach could be adapted to any assembly of chiral (bio)macromolecules, with key advantages in detecting large-scale assemblies with high specificity to aligned and chiral molecules, and improved sensitivity compared to conventional techniques.

KEYWORDS. Chirality; Collagen; Oriented linear dichroism; Hierarchical organization

INTRODUCTION. Processing type I collagen (here *collagen*) as biomaterials is very attractive for tissue engineering and regenerative medicine. It is the main constituent of the extracellular matrix and its hierarchical organization provides tissues with their specific properties and functions. The hierarchical nature of collagen assemblies makes the development of multiscale approaches essential to fully characterize collagen-based tissues and materials. These have largely involved imaging techniques from electron[1,2] to multiphoton microscopy based on second-harmonic generation (SHG), which is considered the gold standard technique for structural imaging of type I collagen assemblies,[3-6] as well as scattering techniques such as small angle X-ray scattering (SAXS).[7-14] UV circular dichroism (CD) is also routinely used to obtain structural information on chiral molecules, typically proteins.[15] Measuring the difference in absorption of left and right circularly polarized light, CD is probably the simplest technique for non-destructively probing of native conformations such as the helical collagen monomer. Specifically, CD reports on local chiral structures that cause local coupling of transition dipole moments. Linear dichroism (LD) also relies on locally coupled dipole moments for locations of bands and intensities. However, LD differs in that it measures the difference of linearly polarized light absorbance

between orientations parallel and perpendicular to an orientation axis. As a result, LD additionally depends on the net orientation of transition moments, offering insights into local structures relative to the long axis of any given structure.[15] In other words, a molecular system yields a LD spectrum only if the chromophore is oriented with respect to the polarization of the incident light.

LD has been used to investigate the structure of biomolecules including nucleic acids and DNA,[16-19] peptides and proteins, their interactions with ligands[15] and their orientation in bilayered membrane systems[20] as reviewed by Rodger and colleagues.[21,22] LD investigations also concern the kinetics of DNA degradation and of protein fiber assembly and disassembly in solution.[23,24] These studies are based on the orientation of molecules in solution. The advancements in Couette flow LD cells[25,26] and the use of stretchable polymer films[27,28] have enabled this progress. These innovations have transformed LD into an effective tool in synthetic biology, facilitating tasks like engineering biological assays for DNA detection through bacteriophage utilization.[29-31] LD has also made a timid breakthrough in the field of supramolecular chemistry, where the characterization of higher-order structures remains an important issue. Carter et al. have recently reported on the use of LD to characterize the flow-induced orientation of foldamers.[32] Apart from that, LD has rarely been used in the dense state, and to our knowledge, has never been applied for the characterization of dense biomaterials, including collagen assemblies, except in theoretical approaches.[33]

To produce thin and dense collagen materials, an acidic solution of collagen was cast in a mold before solvent evaporation. The resulting dense collagen film was then removed from the mold and analyzed by SHG microscopy and SAXS, which revealed a high degree of ordering in the triple helices. Further characterization with synchrotron-radiation angle-resolved linear dichroism (ALD) confirms this high order at the supramolecular level, providing a specific ALD signature

on a larger scale compared to SHG and with improved sensitivity towards organic materials compared to SAXS. In addition, this signature can be readily used to investigate the ordering of triple helices in biomaterials with varying densities, while simultaneously assessing the native conformation of collagen triple helices in the biomaterials *in situ* and in a non-destructive manner.

EXPERIMENTAL SECTION.

Collagen extraction and purification. Type I collagen was extracted and purified from rat tail tendons as previously described by substituting 500 mM acetic acid with 3 mM hydrochloric acid.[13,34] Collagen purity was assessed by electrophoresis and its concentration estimated by hydroxyproline titration.[35] All other chemicals were purchased and used as received. Water was purified with a Direct-Q system (Millipore Co.).

Collagen casting. Collagen films were prepared by pouring 1.2 mL of an acidic solution of collagen (1.7 $mg.ml^{-1}$) in 3 mM HCl in a polytetrafluoroethylene (PTFE) mold (3.5 cm in diameter). The solvent was allowed to evaporate overnight under ambient conditions. The bulk collagen was detached from the mold as transparent dry collagen films.

Second harmonic generation (SHG). We used a custom-built laser-scanning multiphoton microscope and recorded SHG images as previously described.[3,5,6] Excitation was provided by a femtosecond titanium–sapphire laser (Mai-Tai, Spectra-Physics) tuned to 860 nm, scanned in the XY directions using galvanometric mirrors and focused using a 25× with 1.05 NA objective lens (XLPLN25X-WMP2, Olympus), yielding a resolution of 0.35 μm (lateral) × 1.2 μm (axial). Acquisitions were conducted at a frame rate of 100 kHz, with a latera pixel size of 280 nm, and a typical laser power of 12 mW. We used circular polarizations in order to image all structures independently of their orientation in the image plane, and accumulated 4 images per Z position

with a 1 μm Z-step. The Z-stack covered a total depth of 20 μm and was subsequently projected using maximum intensity projection to flatten the membrane image into a single plane.

Small angle X-ray scattering (SAXS). SAXS experiments were performed at 25 °C on the SWING beamline at the Soleil synchrotron facility (Saint-Aubin, France). The samples were analyzed using a beam with an energy of 12.00 keV and a sample-to-detector distance of 2.00 m. The samples were prepared ex situ, pushed through a 1.5 mm quartz capillary (20 μm wall thickness) with a 1 mL syringe and analyzed directly by setting them in front of the X-ray beam. The signal at the same position of the quartz capillary filled with water was subtracted as background. The signal was integrated azimuthally using the local software Foxtrot[36] to obtain the I(q) *vs*. q curves ($q = 4\pi \sin\theta/\lambda$, where 2θ is the scattering angle and $\lambda = 1.03$ Å^{-1} is the X-ray wavelength) after masking wrong pixels and the beam stop shadow. Silver behenate (d(001) = 58.38 Å) was used as SAXS standard to calibrate the sample to detector distance. Data were not scaled to absolute intensity.

Synchrotron-radiation circular dichroism (CD). 25 μL of collagen solutions in 3 mM HCl were loaded in quartz cells (Hellma) with a path length of 0.01 cm. The measurements were performed on the DISCO Beamline at Synchrotron SOLEIL (Saint Aubin, France) during runs No. 20180440 and 20200233.[37,38] For CD acquisitions, raw spectra were acquired from 320 to 170 nm with 1 nm spectral resolution. Three spectra were averaged and processed with the CDTool software.[39] The baseline (HCl 3 mM acquired in the same conditions) was subtracted from them. Intensity calibration was obtained with a camphorsulfonic acid sample.

Synchrotron-radiation linear dichroism (LD). Collagen dry films obtained by solvent evaporation were placed in between two quartz slides with a path length of 0.01 cm in a round

sample holder enabling motorized rotation in the plane perpendicular to the beam with steps of 22.5° over 360°. The LD acquisition was calibrated with naphthalene film as previously described.[38] LD spectra were acquired on the DISCO Beamline at Synchrotron SOLEIL (Saint Aubin, France) from 320 to 170 nm with a 1 nm spectral resolution, setting the modulator to 0.608 x λ and doubling the Lock-in amplifier frequency. Spectra were treated with the CDTool software.[38]

RESULTS AND DISCUSSION.

Collagen can schematically be described as a rod-like particle with high aspect ratio, measuring approximately 300 nm in length and 1.5 nm in diameter. The non-centrosymmetric supramolecular organization of the dipolar peptide bonds along the triple helices results in the generation of an efficient second harmonic signal upon 2-photon excitation of collagen-based assemblies, as observed in tissues. SHG imaging of the dry films obtained through solvent evaporation (Figure 1D) produces an intense signal, as observed in Figure 1A. This signal specifically indicates non-centrosymmetric packing of collagen triple helices within the dry film.

The organization of collagen triple helices in the dry films was then studied using SAXS. The SAXS profile reveals diffraction patterns in the q range 0.1 to 0.7 $Å^{-1}$ indicating the existence of crystalline domains (Figure 1B). This demonstrates a lateral high order packing of the triple helices in the cast film. In tissues, collagen self-assembles into fibrils, which resemble smectic liquid crystal with long-range axial order (where collagen molecules are staggered axially by integral multiples of D = 67 nm),[7,8] but only exhibits short-range order in the lateral direction (i.e., within a plane perpendicular to the fibril axis).[9] We did not investigate correlation distances below q of 0.1, as our focus was on inter-helix interactions rather than collagen fibrillogenesis. A broad correlation peak is observed at 0.54 $Å^{-1}$, corresponding to an inter-helix lateral order with a

distance (d_{Bragg}) of $2\pi/q$ equal to 1.16 nm (Figure 1E). This spacing is characteristic of the arrangement of triple helices in collagen fibrils, as observed in highly organized living tissues such as tendons[9-11] and dense collagen assemblies *in vitro*.[12-14] The large width of the peak indicates that local positional order only extends to nearest neighbors, with a positional correlation length, ξ ($2\pi/\Delta q$) (with Δq the peak's FWHM) of *ca* 7.6 nm.[12,40]

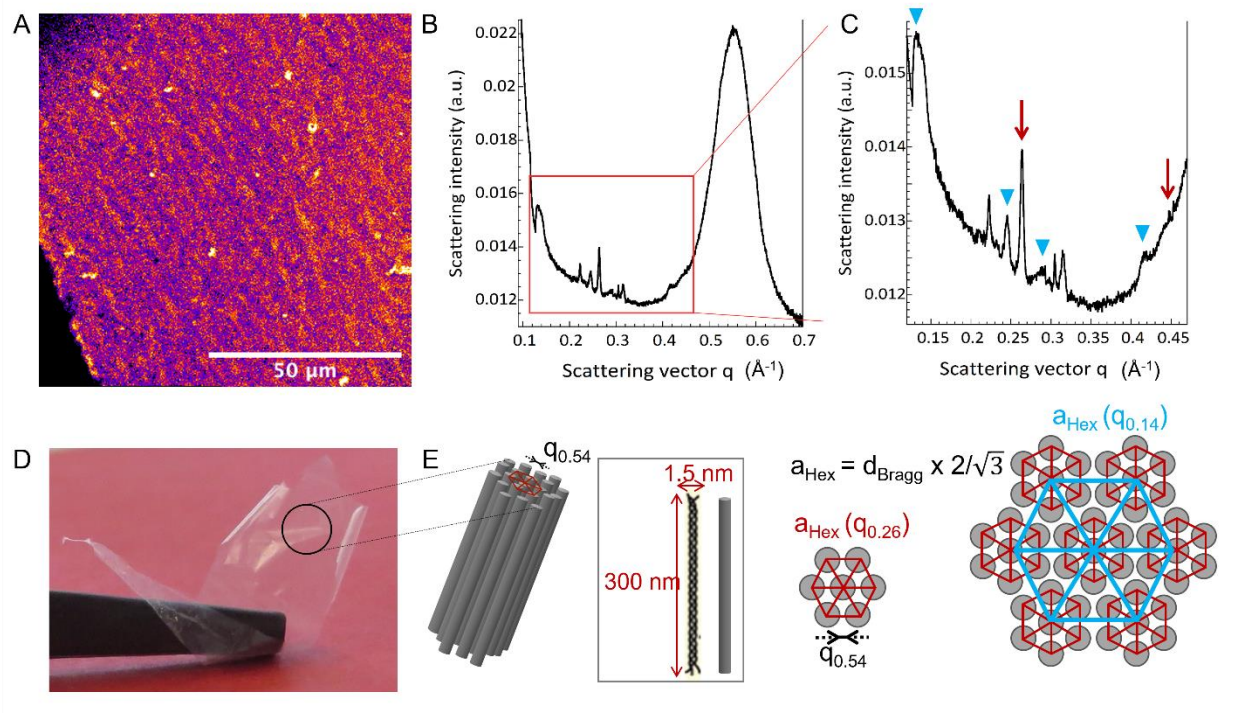

Figure 1. (A) SHG image, (B-C) SAXS diffractogram and (D) photo of the cast collagen film. (E) Schematic of triple helices organization within the cast film.

The SAXS profile also shows sharper Bragg peaks. Some of them can be attributed to six orders of the same fundamental Bragg peak, with a respective q/q_1 ratio of 1, $\sqrt{3}$, 2, $\sqrt{7}$, 3, $2\sqrt{3}$ at 0.14, 0.24, 0.29, (x), 0.42 $Å^{-1}$, and an expected final peak at 0.48 $Å^{-1}$, which we suggest is hidden due to the large width of the peak at 0.54 $Å^{-1}$ (blue triangles, Figure 1C). Based on this analysis, we conclude that the evaporation of organic solvent from an acidic solution of collagen triple helices

yields a hexagonal order in the plane normal to the triple helices, with a hexagonal lattice parameter a_{Hex} of 5.18 nm (with $a_{Hex} = d_1 \times 2/\sqrt{3}$ and $d_1 = 4.49$ nm for $q_1 = 0.14$ Å^{-1}).[40-44] Other Bragg peaks in this area can be attributed to the co-existence of hexagonal domains with different lattice parameters. Correlations between peaks at 0.26, 0.45 and 0.54 Å^{-1} can be identified with q/q_1 ratio of 1, $\sqrt{3}$, 2, with a hexagonal lattice parameter a_{Hex} of 2.79 nm ($q_1 = 0.26$ Å^{-1}) (red arrows, Figure 1C). We attribute the coexistence of the two hexagonal lattice parameters to the hexagonal ordering (a_{Hex} ($q_{0.14}$)) of hexagonal first-order molecular groups (a_{Hex} ($q_{0.26}$)) as described by Hulmes[45] (Figure 1E).

The chirality of molecules broadens the range of characterization techniques, taking advantage of the property of left- and right-circular polarized light to interact with asymmetric chiral objects. CD measurements are routinely used for the characterization of the conformation of biomolecules, typically DNA and proteins. At the supramolecular level, chirality can also be exploited by using LD to extract information on the interactions of chiral (bio)molecules with respect to each other. Collagen solutions and dense films were characterized by synchrotron radiation CD and LD. In solution, CD gives the molecular signature of native collagen, with a large negative band at 198 nm and a smaller positive band at 223 nm (Figure 2A, black plain line). These bands are attributed to the $n \rightarrow \pi^*$ and $\pi \rightarrow \pi^*$ transitions associated with the triple helix of collagen and are characteristic of the polyproline II (PPII) conformation of collagen triple helix.[6,33] However, the corresponding LD spectrum (blue dotted line) shows no signal, attributed to the lack of supramolecular interactions between triple helices in the soluble state. Subsequently, a collagen cast film was placed in the sample holder and CD spectrum acquired. The collagen CD signature, featuring a large negative band at 198 nm and a small positive band at 223 nm (Figure 2B, black plain line),

was once again observed. Upon orienting collagen triple helices, LD absorption is expected at these wavelengths. Indeed, strong LD signals were measured, manifesting as one large band at 203 nm and a smaller one at 185 nm (Figure 2B, blue dotted line).

ALD measurements involved rotating the sample relative to the beam (every 22.5° over 360°), in the plane of the collagen film, perpendicular to the beam propagation direction (Figure 2C). Throughout sample rotation, the bands at 185 and 203 nm were preserved, albeit with varying intensities, ranging from a positive maximum to a negative maximum, passing through the extinction of the ALD signal (Figure 2D). This simultaneous variation in intensity for both bands resulted in two isobestic points (at 182 and 190 nm). Sharp isobestic points are considered as proof for homogeneity of the sample, where triple helices adopt the same configuration, in absence of bundles of different sizes, which would contribute to varying domains sizes and absorption properties.

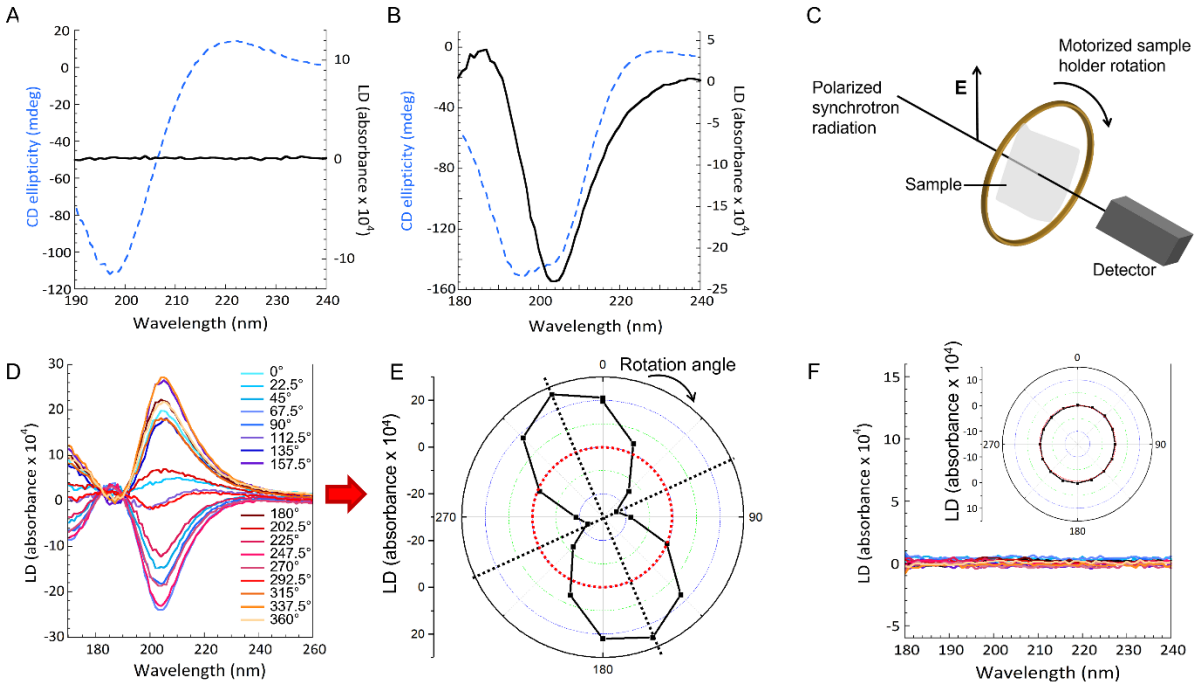

Figure 2. CD and LD spectra (blue dotted and black plain lines respectively) of (A) soluble collagen in 3 mM HCl and (B) collagen in cast film. (C) Schematic of the ALD setup showing the sample holder rotation in the plane normal to the beam propagation direction. (D) ALD spectra of the cast collagen film with varying sample orientation by step of 22.5° over 360 °C with respect to the beam and (E) corresponding polar representation of the maximum intensity of the LD spectrum at each angle as a function of sample orientation (angle of rotation). (F) ALD spectra of soluble collagen and corresponding polar representation (inset). The red-dotted line in ALD polar plots represents the zero LD ellipticity.

The variation of ALD intensity as a function of the relative orientation of the sample and the beam is better shown through a polar representation. Figure 2E is the plot of LD maximum intensity against the rotation angle, with the red dotted line representing zero LD intensity. This polar plot highlights the periodicity of the signal with two distinct lobes: LD is maximized when the sample is highly oriented, with its electric dipole moment aligned parallel to the light polarization direction, then decreases to zero when perpendicular. Subsequently, it reaches a negative maximum with the same absolute intensity as the previously measured positive maximum upon realignment, and again drops to zero when perpendicular (Figure 2E). This two-lobe pattern originates from the high order and alignment of the collagen triple helices in the film. The presence of two axes of symmetry signifies a unidirectional packing of the triple helices. In contrary, a fully isotropic sample, such as an acidic solution of collagen triple helices, results in the averaging of all LD with zero ellipticity (Figure 2F). The polar signature of such an isotropic sample is a circle (Figure 2F insert). Importantly, collagen ordering probed by ALD extends to a large scale, as the organization of collagen triple helices is averaged over the area of the synchrotron radiation beam, that is a few mm^2.

The relevance of ALD in characterizing collagen packing in dense biomaterials was further assessed using biomaterials with varying collagen concentrations in the starting solution, ranging from 0.5 to 20 mg.ml^{-1} (Figure 3A-D). At a low collagen concentration of 0.5 mg.ml^{-1}, the two-lobes pattern of the polar plot is not observable. Instead, a multilobe profiles is obtained, which is assimilated to a circular anisotropic pattern. We attribute this pattern to an anisotropic organization of the triple helices in the film (Figure 3A). In the case of a dilute solution of collagen triple helices, solvent evaporation alone is insufficient to trigger triple helices ordering. In contrast, the two lobes become more defined with increasing collagen concentration in the starting solution, reaching a well-structured alignment at a starting concentration of 20 mg.ml^{-1} (Figure 3B-D). This shows how the distortion of the polar pattern can be used to probe the ordering of collagen in materials.

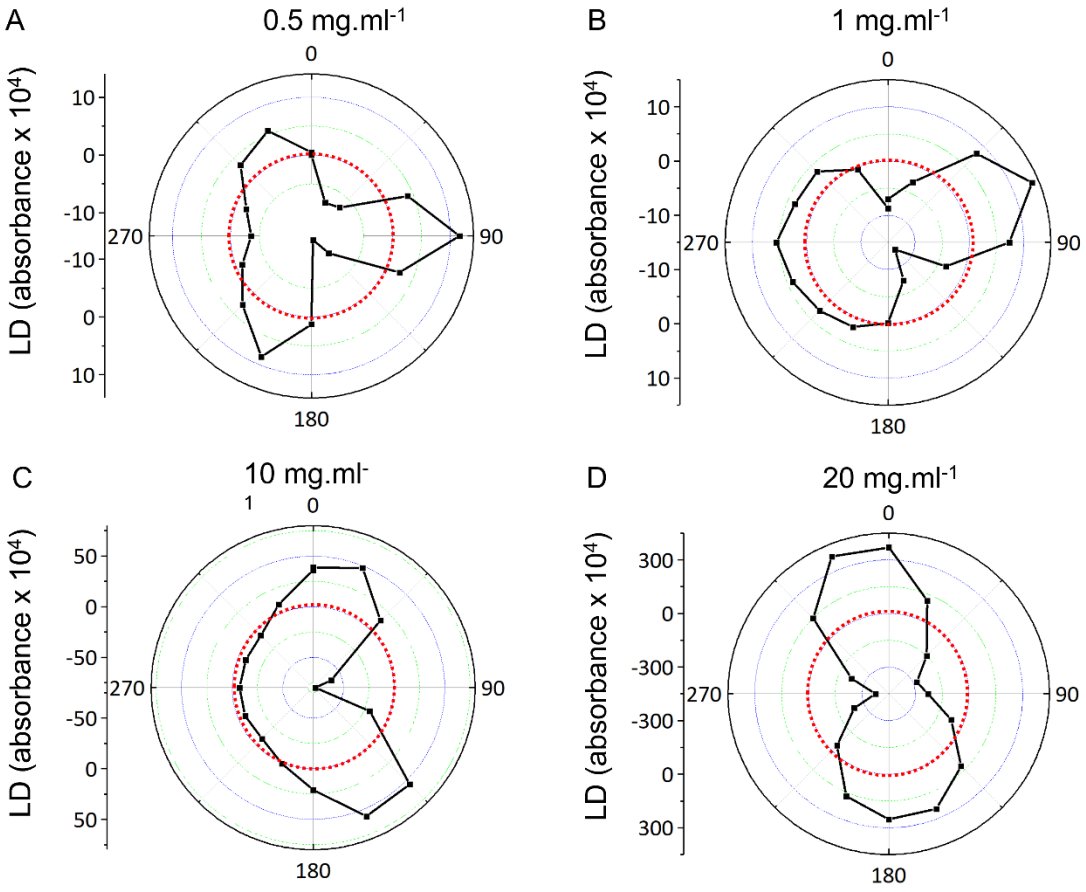

Figure 3. (A-D) ALD polar plots of cast collagen films obtained from collagen solutions of increasing concentrations before casting and solvent evaporation (from 0.5 to 20 $mg.ml^{-1}$). The polar plot corresponds to the maximum intensity of the LD spectrum at each angle as a function of sample orientation (rotation angle by step of 22.5° over 360°, in the plane of the film normal to the beam propagation direction). The red-dotted lines represent the zero LD ellipticity.

To investigate the impact of temperature on collagen conformation within the dense film, the temperature was increased in steps of 4°C from room temperature up to 45°C. The polar plot, in blue, obtained at room temperature is shown in Figure 4. Upon increasing the temperature, we observed a progressive loss of the two-lobes pattern. This phenomenon results from the decrease in intensity at maximum LD ellipticity, which is attributed to the unfolding of collagen triple helices during thermal denaturation (Figure 4A). At 45°C, a circular profile is obtained (plain red line, Figure 4), indicating complete denaturation of collagen triple helices. Above 31°C, the structure is dominated by unordered conformations, and collagen unfolds completely above 40°C. This agrees with previous studies using CD, which determined the melting temperature of collagen to be around 31°C.[6,46] This illustrates that while ALD is used to probe the ordering of collagen within assemblies, it also serves as a means to confirm the native conformation of collagen triple helices within the processed biomaterials and determine the onset of denaturation.

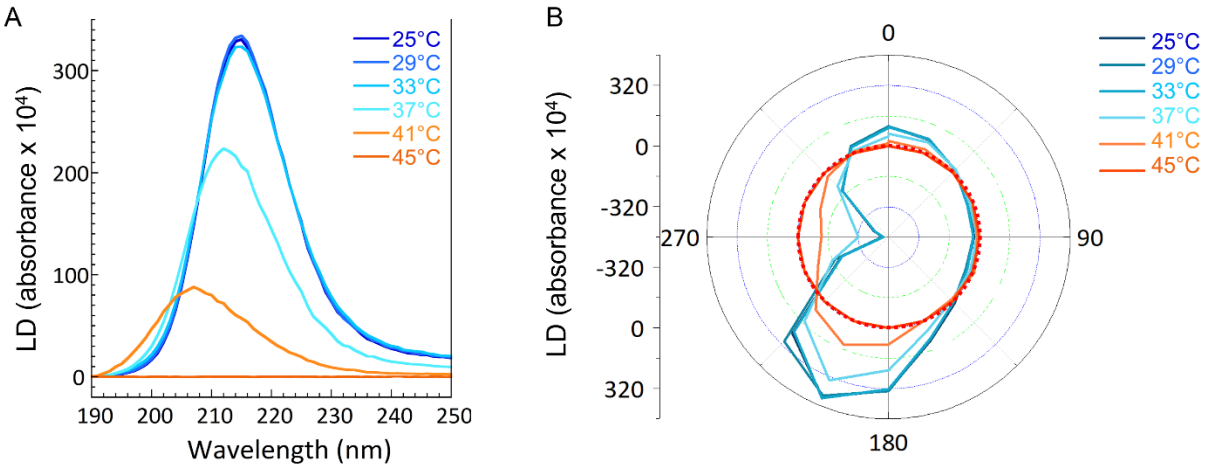

Figure 4. (A) ALD spectra of the cast collagen film upon increasing temperature from 25 to 45°C (corresponding to 180° in (B)), and (B) corresponding polar plots. The polar plot corresponds to the maximum intensity of the LD spectrum at each angle as a function of sample orientation (rotation angle by steps of 22.5° over 360°, in the plane of the film normal to the beam propagation direction). The red-dotted line in ALD polar plots represents the zero LD ellipticity.

CONCLUSION. Here, we used ALD to study the ordering of soluble collagen triple helices after solvent evaporation at room temperature. Our results demonstrate that at a starting concentration of 20 mg.ml^{-1}, collagen triple helices exhibit uniaxial ordering with a hexagonal order, as revealed by combined SHG, SAXS and ALD. We highlight ALD as a highly sensitive and specific method for probing the ordering of chiral objects. By obtaining a polar pattern, we propose a direct assessment of uniaxial ordering through the distortion of the polar pattern. Additionally, ALD provides direct evidence of the preservation of the native helical conformation of the (bio)polymer, which is crucial for biomaterials engineering, particularly in the context of collagen-based biomaterials, where preserving the native triple helix conformation is essential. ALD offers the advantage of probing larger sample areas compared to SHG imaging (mm *vs.* µm), with enhanced

sensitivity towards organic materials compared to SAXS. Furthermore, it is rapid and easily accessible using laboratory CD-equipment, complementing molecular-level CD by providing insights in supramolecular structures and interactions. We anticipate that this methodology can be readily applied to a diverse range of biological or synthetic polymer samples, offering straightforward implementation and data interpretation. We believe that this work will contribute to bridging the gap between the widespread application of (A)LD in supramolecular chemistry, polymers and the field of (bio)materials. Finally, ALD is non-destructive and provides combined information on the conformation, stability and hierarchical organization of native collagen. This information is absolutely essential for tissue engineering and regenerative medicine, as tissue functions are primarily dictated by collagen self-assembly. Consequently, this work will make a new contribution to the characterization and structure-function study of collagen-based assemblies and, more generally, biopolymer-based assemblies of biomedical interest.

ASSOCIATED CONTENT

Supporting Information.

AUTHOR INFORMATION

Corresponding Author

* carole.aime@ens.psl.eu

Author Contributions

The manuscript was written through contributions of all authors. All authors have given approval to the final version of the manuscript.

Funding Sources

We thank the Soleil Synchrotron facility for making available the DISCO and SWING beamline and financial support (proposal No. 20180440, 20200233 and 20201747).

Notes

The authors declare no competing financial interest.

ACKNOWLEDGMENT

We thank François Hache and Pascal Changenet for very helpful discussions. Synchrotron radiation CD and (A)LD on DISCO beamline, and SAXS on SWING beamline at the SOLEIL Synchrotron were performed under proposals 20180440, 20200233 and 20201747.

ABBREVIATIONS

CD, UV Circular Dichroism; SHG, Second Harmonic Generation; SAXS, Small Angle X-ray scattering; LD, Linear Dichroism; ALD, Angle-resolved Linear Dichroism.

REFERENCES

1 Kadler, K. E.; Baldock, C.; Bella, J.; Boot-Handford, R. P. Collagens at a glance, *J. Cell Sci* **2007**, *120*, 1955-1958.

2 Starborg, T.; Kalson, N. S.; Lu, Y.; Mironov, A.; Cootes, T. F.; Holmes, D. F.; Kadler, K. E. Using transmission electron microscopy and 3View to determine collagen fibril size and three-dimensional organization. *Nat Protoc.* **2013**, *8*, 1433-1448.

3 Pena, A. M.; Boulesteix, T.; Dartigalongue, T.; Schanne-Klein, M. C. Chiroptical Effects in the Second Harmonic Signal of Collagens I and IV. *J. Am. Chem. Soc.* **2005**, *127*, 10314-10322.

4 Chen, X.; Nadiarynkh, O.; Plotnikov, S.; Campagnola, P. J. Second harmonic generation microscopy for quantitative analysis of collagen fibrillar structure. *Nat Protoc.* **2012**, *7*, 654-669.

5 Bancelin, S.; Aimé, C.; Gusachenko, I.; Kowalczuk, L.; Latour, G.; Coradin, T.; Schanne-Klein, M.-C. Determination of collagen fibrils size via absolute measurements of Second Harmonic Generation signals. *Nat Commun.* **2014**, *5*, 4920.

6 Dems, D.; Rodrigues Da Silva, J.; Helary, C.; Wien, F.; Marchand, M.; Debons, N.; Muller, L.; Chen, Y.; Schanne-Klein, M.-C.; Laberty-Robert, C.; Krins, N.; Aimé, C. Native collagen: electrospinning of pure, cross-linker free self-supported membrane. *ACS Appl Bio Mater*, **2020**, *3*, 2948-2957.

7 Goh, K. L.; Hiller, J.; Haston, J. L.; Holmes, D. F.; Kadler, K. E.; Murdoch, A.; Meakin, J. R.; Wess, T. J. Analysis of collagen fibril diameter distribution in connective tissues using small-angle X-ray scattering. *Biochim Biophys Acta*, **2005**, *1722*, 183-188.

8 Basil-Jones, M. M.; Edmonds, R. L.; Allsop, T. F.; Cooper, S. M.; Holmes, G.; Norris, G.E.; Cookson, D. J.; Kirby, N.; Haverkamp, R. G. Leather Structure Determination by Small-Angle X-ray Scattering (SAXS): Cross Sections of Ovine and Bovine Leather. *J. Agric. Food Chem.* **2010**, *58*, 5286-5291.

9 Hulmes, D. J. S.; Wess, T. J.; Prockop, D. J.; Fratzl, P. Radial Packing, Order, and Disorder in Collagen Fibrils. *Biophys J.* **1995**, *68*, 1661-1670.

10 Hulmes, D. J. S.; Miller, A. Quasi-hexagonal molecular packing in collagen fibrils. *Nature* **1979**, *282*, 878-880.

11 Fraser, R. D. B.; MacRae, T. P.; Miller, A.; Suzuki, E. Molecular Conformation and Packing in Collagen Fibrils. *J. Mol. Biol.* **1983**, *167*, 497-521.

12 Gobeaux, F.; Belamie, E.; Mosser, G.; Davidson, P.; Panine, P.; Giraud-Guille, M. M. Cooperative ordering of collagen triple helices in the dense state. *Langmuir* **2007**, *23*, 6411-6417.

13 Gobeaux, F.; Mosser, G.; Anglo, A.; Panine, P.; Davidson, P.; Giraud-Guille, M. M.; Belamie, E. Fibrillogenesis in dense collagen solutions: a physicochemical study. *J. Mol. Biol.* **2008**, *376*, 1509-1522.

14 Nassif, N.; Gobeaux, F.; Seto, J.; Belamie, E.; Davidson, P.; Panine, P.; Mosser, G.; Fratzl, P.; Giraud-Guille, M. M. *Chem. Mater.* **2010**, *22*, 3307-3309.

15 Daviter, T.; Chmel, N.; Rodger, A. Circular and linear dichroism spectroscopy for the study of protein-ligand interactions. *Methods Mol Biol.* **2013**, *1008*, 211-241.

16 Clack, B. A.; Gray, D. M. Flow Linear Dichroism Spectra of Four Filamentous Bacteriophages: DNA and Coat Protein Contributions. *Biopolymers* **1992**, *32*, 795−810.

17 Rittman, M.; Hoffmann, S. V.; Gilroy, E.; Hicks, M. R.; Finkenstadt, B.; Rodger, A. Probing the Structure of Long DNA Molecules in Solution Using Synchrotron Radiation Linear Dichroism. *Phys. Chem. Chem. Phys.* **2012**, *14*, 353−366.

18 Nordén, B.; Kurucsev, T. Analysing DNA Complexes by Circular and Linear Dichroism. *J. Mol. Recognit.* **1994**, *7*, 141−155.

19 Norden, B.; Kubista, M.; Kurucsev, T. Linear Dichroism Spectroscopy of Nucleic Acids. *Q. Rev. Biophys.* **1992**, *25*, 51-170.

20 Lanphere, C.; Ciccone, J.; Dorey, A.; Hagleitner-Ertuğrul, N.; Knyazev, D.; Haider, S.; Howorka, S. Triggered Assembly of a DNA-Based Membrane Channel. *J Am Chem Soc.* **2022**, *144*, 4333-4344.

21 Hicks, M. R.; Kowałski, J.; Rodger, A. LD Spectroscopy of Natural and Synthetic Biomaterials. *Chem. Soc. Rev.* **2010**, *39*, 3380.

22 Rodger, A.; Dorrington, G.; Ang, D. L. Linear dichroism as a probe of molecular structure and interactions. *Analyst* **2016**, *141*, 6490−6498.

23 Bromley, E. H. C.; Channon, K. J.; King, P. J. S.; Mahmoud, Z. N.; Banwell, E. F.; Butler, M. F.; Crump, M. P.; Dafforn, T. R.; Hicks, M. R.; Hirst, J. D.; Rodger, A.; Woolfson, D. N. Assembly Pathway of a Designed α-Helical Protein Fiber. *Biophys. J.* **2010**, *98*, 1668−1676.

24 Dafforn, T. R.; Rajendra, J.; Halsall, D. J.; Serpell, L. C.; Rodger, A. Protein Fiber Linear Dichroism for Structure Determination and Kinetics in a Low-Volume, Low-Wavelength Couette Flow Cell. *Biophys. J.* **2004**, *86*, 404-410.

25 Marrington, R.; Dafforn, T. R.; Halsall, D. J.; MacDonald, J. I.; Hicks, M.; Rodger, A. Validation of New Microvolume Couette Flow Linear Dichroism Cells. *Analyst* **2005**, *130*, 1608.

26 Hicks, M. R.; Rodger, A.; Lin, Y.-p.; Jones, N. C.; Hoffmann, S. V.; Dafforn, T. R. Rapid Injection Linear Dichroism for Studying the Kinetics of Biological Processes. *Anal. Chem.* **2012**, *84*, 6561−6566.

27 Razmkhah, K.; Chmel, N. P.; Gibson, M. I.; Rodger, A. Oxidized Polyethylene Films for Orienting Polar Molecules for Linear Dichroism Spectroscopy. *Analyst* **2014**, *139*, 1372−1382.

28 Tridgett, M.; Moore-Kelly, C.; Duprey, J.-L. H. A.; Iturbe, L. O.; Tsang, C. W.; Little, H. A.; Sandhu, S. K.; Hicks, M. R.; Dafforn, T. R.; Rodger, A. Linear Dichroism of Visible-Region Chromophores Using M13 Bacteriophage as an Alignment Scaffold. *RSC Adv.* **2018**, *8*, 29535−29543.

29 Pacheco-Gómez, R.; Kraemer, J.; Stokoe, S.; England, H. J.; Penn, C. W.; Stanley, E.; Rodger, A.; Ward, J.; Hicks, M. R.; Dafforn, T. R. Detection of Pathogenic Bacteria Using a Homogeneous Immunoassay Based on Shear Alignment of Virus Particles and Linear Dichroism. *Anal. Chem.* **2012**, *84*, 91-97.

30 Carr-Smith, J.; Pacheco-Gómez, R.; Little, H. A.; Hicks, M. R.; Sandhu, S.; Steinke, N.; Smith, D. J.; Rodger, A.; Goodchild, S. A.; Lukaszewski, R. A.; Tucker, J. H. R.; Dafforn, T. R. Polymerase Chain Reaction on a Viral Nanoparticle. *ACS Synth. Biol.* **2015**, *4*, 1316−1325.

31 Ali, A.; Little, H. A.; Carter, J. G.; Douglas, C.; Hicks, M. R.; Kenyon, D. M.; Lacomme, C.; Logan, R. T.; Dafforn, T. R.; Tucker, J. H. R. Combining Bacteriophage Engineering and Linear Dichroism Spectroscopy to Produce a DNA Hybridisation Assay. *RSC Chem. Biol.* **2020**, *1*, 449-454.

32 Carter, J. G.; Pfukwa, R.; Riley, L.; Tucker, J. H. R.; Rodger, A.; Dafforn, T. R.; Klumperman, B. Linear Dichroism Activity of Chiral Poly(p-Aryltriazole) Foldamers. *ACS Omega* **2021**, *6*, 33231-33237.

33 Caldwell, J. W.; Applequist, J. Theoretical π-π* Absorption, Circular Dichroic, and Linear Dichroic Spectra of Collagen Triple Helices. *Biopolymers* **1984**, *23*, 1891-1904.

34 Giraud-Guille, M.-M.; Besseau, L.; Herbage, D.; Gounon, P. Optimization of Collagen Liquid-Crystalline Assemblies - Influence of Sonic Fragmentation. *J. Struct. Biol.* **1994**, *113*, 99−106.

35 Bergman, I.; Loxley, R. Two Improved and Simplified Methods for the Spectrophotometric Determination of Hydroxyproline. *Anal. Chem.* **1963**, *35*, 1961−1965.

36 Thureau, A.; Roblin, P.; Perez, J. BioSAXS on the SWING beamline at Synchrotron SOLEIL. *J. Appl. Cryst.* **2021**, *54*, 1698−1710.

37 Giuliani, A.; Jamme, F.; Rouam, V.; Wien, F.; Giorgetta, J.-L.; Lagarde, B.; Chubar, O.; Bac, S.; Yao, I.; Rey, S.; Herbeaux, C.; Marlats, J.-L.; Zerbib, D.; Polack, F.; Réfrégiers, M. DISCO: a low energy multipurpose beamline at synchrotron SOLEIL. *J. Synchrotron Radiat.* **2009**, *16*, 835−841.

38 Wien, F; Paternostre, M; Gobeaux, F; Artzner, F; Refregiers, M. Calibration and quality assurance procedures at the far UV linear and circular dichroism experimental station DISCO. *J. Phys.: Conf. Ser.* **2013**, *425*, 122014.

39 Lees, J. G.; Smith, B. R.; Wien, F.; Miles, A. J.; Wallace, B. A. CDtool-an integrated software package for circular dichroism spectroscopic data processing, analysis, and archiving. *Anal. Biochem.* **2004**, *332*, 285−289.

40 Grelet, E. Hexagonal Order in Crystalline and Columnar Phases of Hard Rods. *Phys. Rev. Lett.* **2008**, *100*, 168301.

41 Hamon, C.; Postic, M.; Mazari, E.; Bizien, T.; Dupuis, C.; Even-Hernandez, P.; Jimenez, A.; Courbin, L.; Gosse, C.; Artzner, F.; Marchi-Artzner, V. Three-dimensional self-assembling of gold nanorods with controlled macroscopic shape and local smectic B order. *ACS Nano* **2012**, *6*, 4137-4146.

42 Loubat, A.; Impéror-Clerc, M.; Pansu, B.; Meneau, F.; Raquet, B.; Viau, G.; Lacroix, L. M. Growth and Self-Assembly of Ultrathin Au Nanowires into Expanded Hexagonal Superlattice Studied by in Situ SAXS. *Langmuir* **2014**, *30*, 4005-4012.

43 Lapkin, D.; Mukharamova, N.; Assalauova, D.; Dubinina, S.; Stellhorn, J.; Westermeier, F.; Lazarev, S.; Sprung, M.; Karg, M.; Vartanyants, I. A.; Meijer, J. M. In situ characterization of crystallization and melting of soft, thermoresponsive microgels by small-angle X-ray scattering. *Soft Matter* **2022**, *18*, 1591-1602.

44 Liu, C. K.; Warr, G. G. Hexagonal closest-packed spheres liquid crystalline phases stabilised by strongly hydrated counterions. *Soft Matter* **2014**, *10*, 83-87.

45 Hulmes, D. J. S. Building Collagen Molecules, Fibrils, and Suprafibrillar Structures. *J Struct Biol* **2002**, *137*, 2-10.

46 Bürck, J.; Heissler, S.; Geckle, U.; Ardakani, M. F.; Schneider, R.; Ulrich, A. S.; Kazanci, M. Resemblance of electrospun collagen nanofibers to their native structure. *Langmuir* **2013**, *29*, 1562−1572.